Journal of Applied Polymer Science

Thermal conductivity and stability of a three-phase blend of carbon nanotubes, conductive polymer, and silver nanoparticles incorporated into polycarbonate nanocomposites

Archana Patole, Isaac Aguilar Ventura, Gilles Lubineau
King Abdullah University of Science and Technology (KAUST), Physical Science and Engineering Division, COHMAS Laboratory, Thuwal, Saudi Arabia
Correspondence to: G. Lubineau (E-mail: gilles.lubineau@kaust.edu.sa)

ABSTRACT: Metallic and non-metallic nanofillers can be used together in the design of polycarbonate (PC) nanocomposites with improved electrical properties. Here, the preparation of three-phase blend (carbon nanotubes (CNT), silver nanoparticles, and conductive polymer) in a two-step process before incorporation in the PC is reported. First, ethylene diamine functionalized multiwall carbon nanotubes (MWCNT-EDA) were decorated with Ag nanoparticles. Next, the Ag-decorated CNTs were coated with poly(3,4-ethylenedioxythiophene) polystyrene sulfonate (PEDOT : PSS). Due to the high thermal conductivity instrinsic to both metallic and non-metallic phases, it is expected that the thermal properties of the resulting nanocomposite would largely differ from those of pristine PC. We thus investigated in detail how this hybrid conductive blend affected properties such as the glass transition temperature, the thermal stability, and the thermal conductivity of the nanocomposite. It was found that this strategy results in improved thermal conductivity and thermal stability of the material. © 2015 Wiley Periodicals, Inc. J. Appl. Polym. Sci. **2015**, *132*, 42281.

KEYWORDS: nanostructured polymers; polycarbonates; thermal properties; thermogravimetric analysis

Received 18 January 2015; accepted 30 March 2015
DOI: 10.1002/app.42281

INTRODUCTION

Polycarbonate (PC) is widely used as a thermoplastic polymer matrix for manufacturing thermally and mechanically superior polymer nanocomposites.[1–4] In particular, fillers, such as inorganic nanoparticles,[5] organic materials,[6] and nanofibrous materials (nanofibers and nanotubes),[7] have been used in conjunction with PC matrices. Among these fillers, multiwall carbon nanotubes (MWCNTs) have received much attention due to their unique mechanical and thermal properties.

Common problems associated with the incorporation of MWCNTs into PC matrices are the poor dispersion of MWCNTs and the weak interfacial strength between MWCNTs and the PC matrix. As a possible solution to solve both problems, much attention has been paid to the MWCNTs, physical, and chemical functionalization.[8,9] In particular, chemical functionalization can be used to create two-phase fillers joined together by a coupling agent. By this technique, MWCNTs can be tailored to improve the properties of a polymer nanocomposite.[10]

Ag nanoparticles decorated on functionalized MWCNTs have already been used as a filler in polymer nanocomposites. Ag is used because it has been shown to improve the inherent thermal properties of MWCNTs. Additionally, nanometer-sized Ag particles on MWCNTs exhibit a dispersion effect in which they efficiently restrict the agglomeration of MWCNTs in a polymer matrix.[11] Different surfactants, such as biomolecules,[12] inorganic particles,[13] and conducting polymers[2] can be used in conjunction with two-phase MWCNT fillers. We are interested in using PEDOT : PSS to create a three-phase filler, due to its inherent stability, high mechanical flexibility, and easy processability, which could ultimately lead to improvements in the electrical, thermal, and mechanical properties of PC nanocomposites.[1,2]

In our previous work, we studied the electrical properties of PC nanocomposites with three-phase fillers, such as Ag nanoparticles attached to amine-modified MWCNTs and further coated with PEDOT : PSS. We observed that the electrical properties of PC nanocomposites with three-phase fillers improved by two orders of magnitude as compared with a single-phase filler (MWCNTs) and by an order of magnitude compared with a two-phase filler (EP-MWCNT).[9] Here, we report on the mechanical and thermal properties of PC nanocomposites with a three-phase filler. Our results demonstrate the internal plasticization effect of PEDOT : PSS in multiphase polymer nanocomposites. We also investigated the role played by PEDOT : PSS-coated Ag nanoparticles in the thermal conductivity and thermal stability of PC nanocomposites. We found that the incorporation of such a three-phase filler in

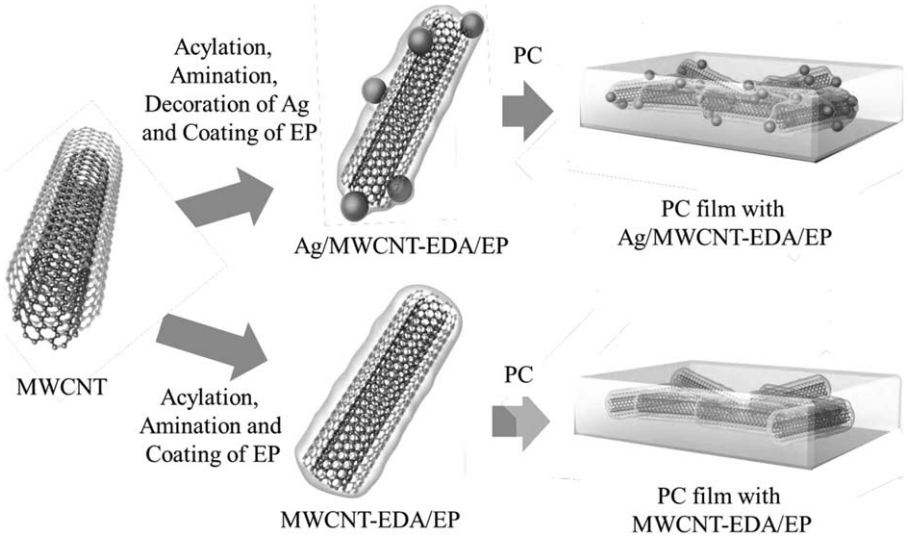

Figure 1. Steps showing the synthesis of PC nanocomposite films loaded with MWCNT-EDA/EP and Ag/MWCNT-EDA/EP fillers. [Color figure can be viewed in the online issue, which is available at wileyonlinelibrary.com.]

the polymer matrix is a viable route to obtain PC nanocomposites with improved thermal properties.

EXPERIMENTAL

Chemicals

SABIC Innovative Plastics supplied the PC (Lexan ML9103-111T) in bead form. Carboxyl functionalized multiwall carbon nanotubes (MWCNT-COOH) with 95% purity and 2.1 g/cm^3 density were purchased from Cheap Tubes. These were produced by catalyzed chemical vapor deposition and had diameters in the range of 8–15 nm and lengths in the range of 10–50 μm. An aqueous dispersion of PEDOT : PSS (Clevios PH1000) was purchased from HC Stark. The initial concentration of PEDOT : PSS was 1.3 wt % and the weight ratio of poly(3,4-ethylenedioxythiophene) (PEDOT) to polystyrene sulfonate (PSS) was 1 : 2.5. Sodium borohydride ($NaBH_4$), Thionyl chloride ($SOCl_2$), Sodium deodecyl sulfate (SDS), Dimethyl formamide (DMF), Dichloromethane (DCM), Tetrahydrofuran (THF), Ethylene glycol (EG), Ethyl alcohol, Acetone, Ethylene diamine (EDA), and Silver nitrate ($AgNO_3$) were purchased from Sigma-Aldrich.

Methods

First, MWCNT-EDA and Ag/MWCNT-EDA precursors were coated with the EG treated PEDOT : PSS conductive polymer blend (EP), to create an Ag/MWCNT-EDA/EP three-phase filler and an MWCNT-EDA/EP two-phase filler. The synthesis recipes to prepare ethylene diamine-decorated MWCNT (MWCNT-EDA) and Ag-decorated diamine functionalized MWCNTs (Ag/MWCNT-EDA) were presented previously.[9] For the coating, different concentrations of (3, 5, 7, and 11 wt %) MWCNT-EDA or Ag/MWCNT-EDA precursors were dispersed into the EP. The mixtures were stirred and sonicated for 15 min in an ice bath. A fixed amount of 11 wt % filler was selected based on its high electrical conductivity reported in our previous work.[9]

To prepare PC nanocomposites, different concentrations (0.5, 1, 1.5, and 2 wt %) of 11 wt % Ag/MWCNT-EDA/EP and MWCNT-EDA/EP fillers were used. To fabricate the nanocomposites, PC beads were first dissolved in DCM and stirred for 5 h at room temperature. Corresponding amounts from the 11 wt % Ag/MWCNT-EDA/EP or the MWCNT-EDA/EP solutions were dispersed in a separate DCM solution. Both, the PC and the MWCNT solutions were then mixed together and stirred for 1 h. The homogeneous mixing of the filler inside the PC matrix was achieved by 10 min of vigorous ultrasonication performed in an ice bath to avoid overheating and to prevent solvent evaporation. PC nanocomposite films were prepared by the cast-coating method and left to dry. Finally, films were formed using a hot press (Pinette Emidecau Ind.) at 240°C and 7 bar pressure for 30 min. Pure PC film, i.e., without fillers, was also prepared in the same way. The overall PC nanocomposite film preparation steps are depicted in Figure 1.

Characterization

Scanning electron microscopy (SEM) was carried out with a Nano Nova 600 (FEI Company). Transmission electron microscopy (TEM) images were captured on a Tecnai Spirit T12 (FEI Company) at an accelerating voltage of 120 kV. Samples were dispersed in ethanol, drop-coated onto a copper grid (Pacific Grid Tech), and dried at room temperature before being loaded into the TEM chamber.

Thermogravimetric analysis (TGA) was performed on a TG 209 F1 instrument (NETZSCH Company) under a nitrogen purge. The sample was heated from 50 to 800°C at a heating rate of 10°C/min. Three samples of each formulation were tested. We present the results from a single, most representative specimen per each configuration.

Differential scanning calorimetry (DSC) analysis was carried out using a TG 204 F1 instrument (NETZSCH Company) under a nitrogen purge. The samples were heated from 30 to 250°C at 10°C/min. Only one sample per configuration was tested.

The temperature-dependent thermal conductivity, K (W m^{-1} K^{-1}), of the samples was calculated as:[14]

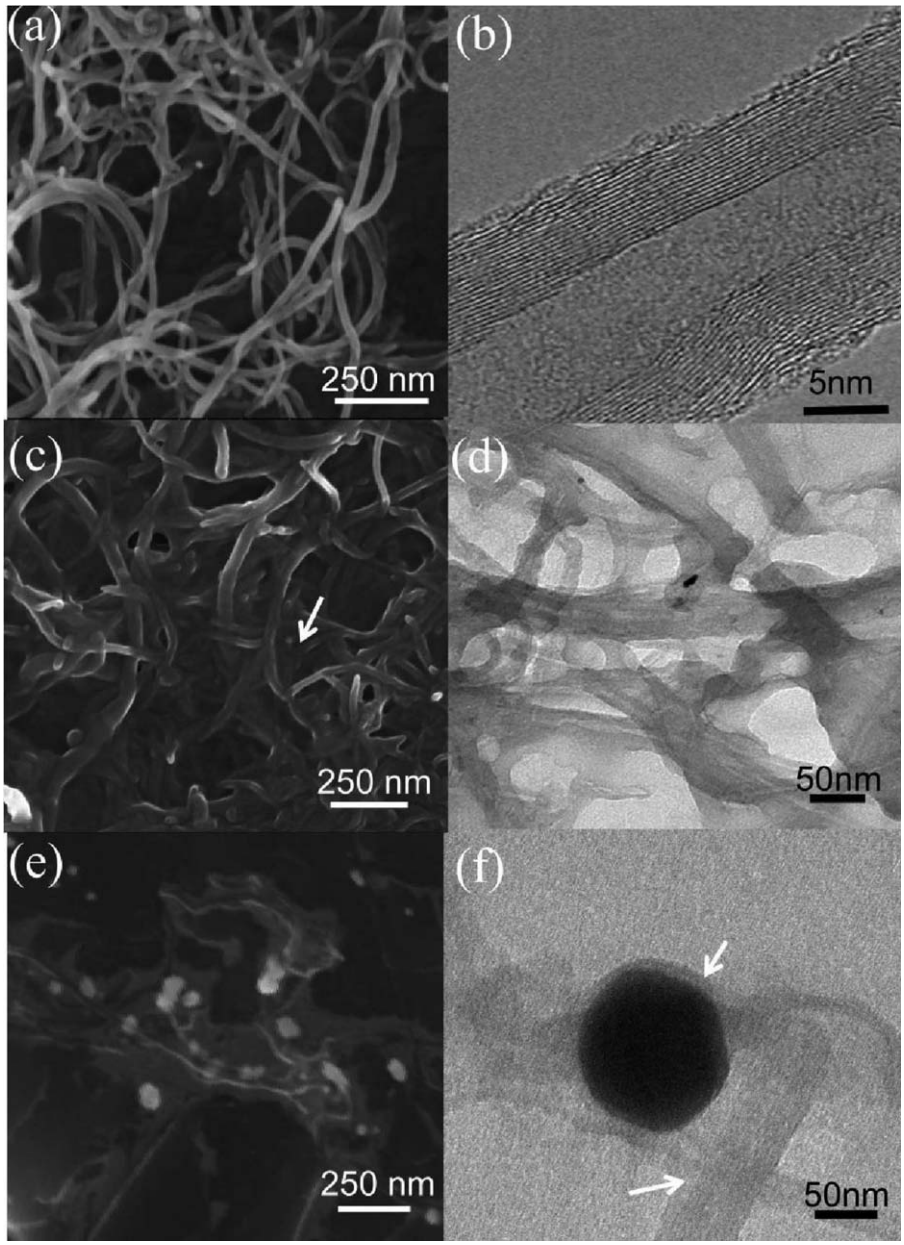

Figure 2. Morphologies of nanofillers : SEM (left column) and TEM (right column) images of MWCNT-COOH (a, b), MWCNT-EDA/EP (c, d), and Ag/MWCNT-EDA/EP (d, e). Arrows indicate the coating of PEDOT : PSS on the MWCNT.

$$K\ (T) = a(T) * Cp(T) * \rho\ (T) \quad (1)$$

where α is the thermal diffusivity ($m^2\ s^{-1}$), Cp is the specific heat (J $kg^{-1}\ K^{-1}$), and ρ is the bulk density (kg m^{-3}) of the samples.

Thermal diffusivity was measured using disc-shaped samples (12.6±0.05 mm in diameter and 1.4±0.05 mm in thickness) and a LFA 447 Nanoflash instrument (NETZSCH Company), which is based on the flash method. Five measurements were performed at each temperature (50, 75, 100, and 120°C). We report the average value and standard deviation for each case. Each sample was coated with graphite before testing.

The Cp of the samples was obtained from the DSC curves by using the ratio method:[15]

$$C_{P_{Sample}}(\mathrm{T}) = \frac{H_{Sample}}{H_{Standard}} * \frac{M_{Standard}}{M_{Sample}} * C_{P_{Standard}} \quad (2)$$

where H is the heat flow (mW) and M is the mass (mg). Sapphire was used as a standard and the temperature range was 25 to 140°C. Finally, the density was evaluated using a Discovery Density Determination Kit (Ohaus) only at room temperature and was assumed constant for the calculation of thermal conductivity at different temperatures.

Dynamic mechanical analysis (DMA) was performed on a DMA 242 C instrument (NETZSCH Company) in tension mode. Rectangular samples of PC and PC nanocomposite films with 10 × 5 × 0.2 mm dimensions were prepared. The measurements were carried out in the temperature range of 25 to 180°C at a

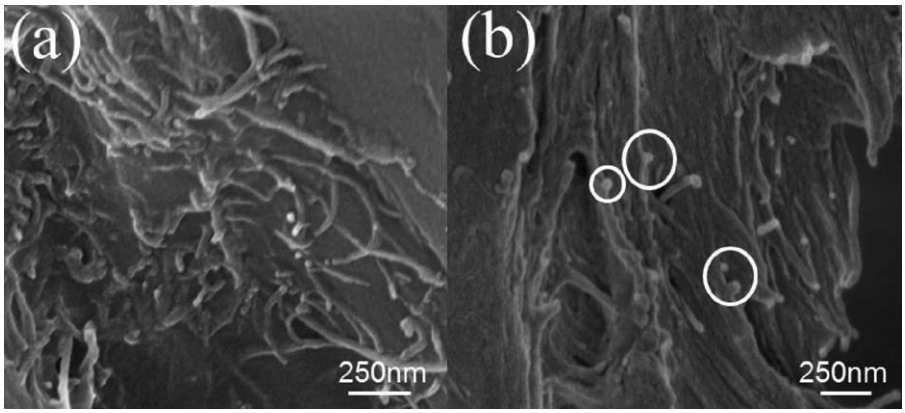

Figure 3. SEM images of (a) an MWCNT-EDA/EP/PC nanocomposite and (b) an Ag/MWCNT-EDA/EP/PC nanocomposite. Ag nanoparticles on MWCNT are highlighted with red circles.

heating rate of 10°C/min in a nitrogen enviroment and at 10 Hz frequency. The relative humidity was around 60% in the test chamber. Three samples of each formulation were tested. We report the results from a single, most representative specimen respectively.

Tensile properties were measured by using an Instron 5882 equipped with a 500 N load cell. Rectangular samples (45 mm × 15 mm × 0.25 mm) were prepared and tested with a 1 mm/min extension rate. Young's moduli were measured as the slope in the initial straight portion of the stress-strain curve below 0.05% of the longitudinal strain. Five samples for each specimen were measured. All reported values are an average of five test results.

RESULTS AND DISCUSSION

Morphology of MWCNT-EDA/EP, Ag/MWCNT-EDA/EP, and PC Nanocomposites

Figure 2(a,b) show SEM and TEM images of pristine MWCNT-COOH.[16] The average diameter of these uncoated MWCNTs measured in the TEM image is about 15 nm. The diameter of the MWCNTs increased to 50–60 nm after they were coated with EG treated PEDOT : PSS [Figure 2(c)], indicating that the nanotubes were well coated by the conductive polymer. The coating appears to be quite uniform with the diameter fluctuation observed by under TEM less than 5 nm [see Figure 2(d)]. We note that the EP coating plays an important role in improving the microstructure of the conductive blend as it behaves as a dispersing agent and helps to individualize the MWCNTs.[9] The MWCNTs appear to be well individualized when they are decorated by Ag nanoparticles before coating with EP. In Figure 2(e), well indiviualized MWCNTs, decorated with Ag nanoparticles can be seen. These Ag nanoparticles are around 100 nm in diameter and might help to separate the MWCNTs in the final compound due to their large scale in comparision with the diameter of the MWCNTs [Figure 2(f)]. It is possible to see that Ag nanoparticles are not only decorated on the MWCNTs but also remotely isolated in the form of small clusters in the EP matrix. Figure 3(a,b) show SEM images of 2 wt % MWCNT-EDA/EP/PC and 2 wt % Ag/MWCNT-EDA/EP/PC nanocomposites. It is noteworthy to mention that even at the higher concentration (2 wt %), the MWCNTs are well distributed in the matrix without any agglomeration.

Thermal Stability of Individual Precursors

To compare the effect of Ag/MWCNT-EDA/EP and MWCNT-EDA/EP on the thermal stability of PC nanocomposites, the thermal degradation behavior of the individual precursors was studied. Figure 4 shows the thermal degradation of MWCNT-COOH, MWCNT-EDA, and PC. MWCNT-COOH exhibit a 2.15 wt % degradation from 150 to 600°C attributed to the loss of COOH. In MWCNT-EDA, EDA starts to degrade at 180°C and completely degrades at 300°C contributing to the overall loss of around 45 wt %. PC starts degrading at 430°C, which is mainly initiated by the preliminary thermal scission of the C–C bonds and the formation of gases such as CO and CO_2.[17]

Thermal Degradation of PC Nanocomposites

In this section, we analyze the thermal degradation behavior of the three-phase filler/PC nanocomposites. To understand the relationships between each phase of the material and the PC

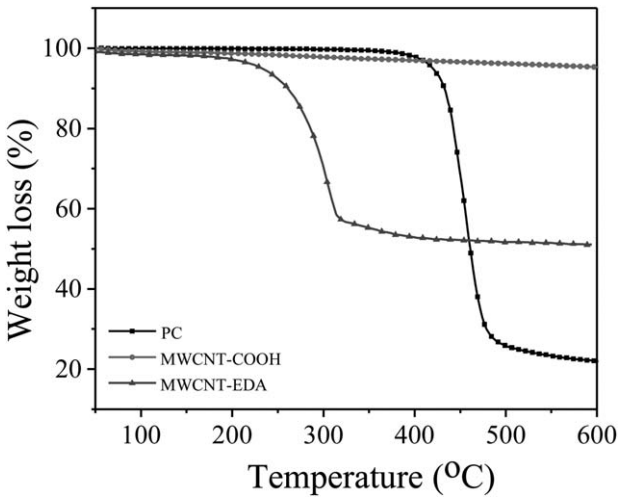

Figure 4. TGA curves of PC, MWCNT-COOH and MWCNT-EDA. [Color figure can be viewed in the online issue, which is available at wileyonlinelibrary.com.]

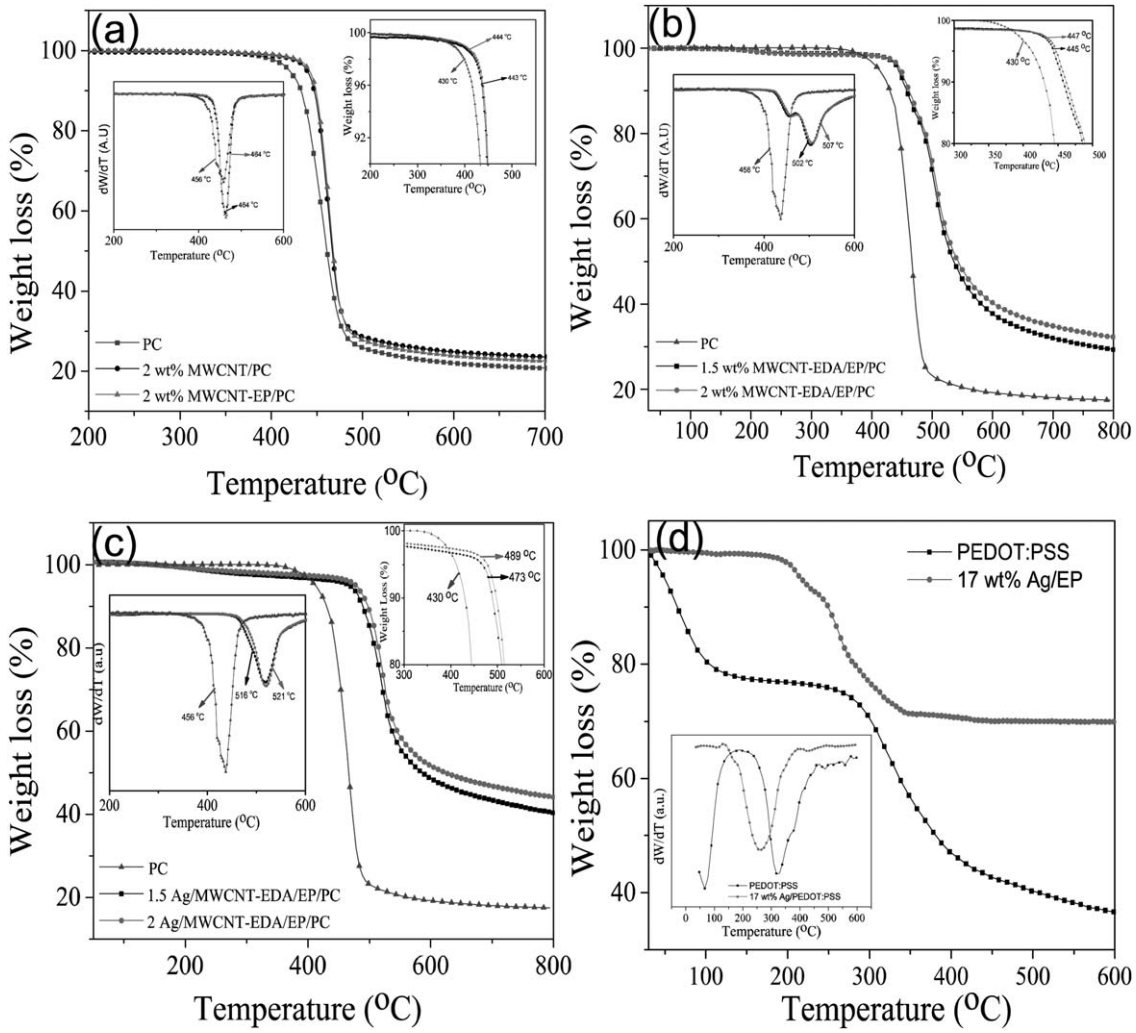

Figure 5. TGA curves of (a) 2 wt % of MWCNT/PC and MWCNT-EP/PC nanocomposites, (b) 1.5 and 2 wt % of MWCNT-EDA/EP/PC nanocomposite, (c) 1.5 and 2 wt % of Ag/MWCNT-EDA/EP/PC nanocomposite, and (d) PEDOT : PSS and 17 wt % of Ag/EP. Respective DTA peaks are shown in the inset of all TGA analysis. [Color figure can be viewed in the online issue, which is available at wileyonlinelibrary.com.]

matrix, we systematically prepared nanocomposites adding one phase at a time.

First, we study the effect of –COOH-functionalized MWCNTs and the EP-coated MWCNTs in PC with a fixed 2 wt % MWCNT concentration. The thermal degradation profile of these samples, also studied in our previous report,[1] is shown in Figure 5(a). From the insets in Figure 5(a), we can identify the thermal onset temperature (T_{onset}) and the temperature at which the degradation rate is maximum (T_d) in pristine PC and nanocomposites. T_{onset} and T_d are observed at 443 and 464°C for 2 wt % MWCNT/PC, whereas they are at 444 and 464°C for 2 wt % MWCNT/EP/PC. T_{onset} and T_d are nearly the same for the both nanocomposites. Here, we also note that, despite the existence of an hydrogen bond between EP and PC,[1] the thermal stability of PC nanocomposites was not significantly improved due to the coating of EP on MWCNT. However, both samples clearly show an improvement in the thermal conductivity over pristine PC. For example, T_{onset} increased by 14°C and T_d by around 8°C for 2 wt % MWCNT-EP/PC samples as compared with PC. We ascribe this modification to the barrier effect caused by the presence of MWCNTs in the PC. In this sense, MWCNTs obstruct the transport of PC chains, delaying the decomposition towards higher temperatures.

Secondly, we study the effect of using MWCNT-EDA/EP instead of the original –COOH functionalized MWCNTs used in the previous samples. Figure 5(b) shows thermal degradation profiles of PC nanocomposites at 1.5 and 2 wt % MWCNT-EDA/EP/PC. For both nanocomposites, the initial 2 wt % weight loss observed at 200–400°C can be attributed to the degradation of EDA as shown in Figure 4. As before, the presence of MWCNTs increases the T_{onset} and T_d as compared to pristine PC. Nevertheless, we observe a two-step degradation profile between 400 and 600°C. The main degradation happens at $T_{onset} = 445$°C and $T_d = 502$°C for the 1.5 wt % MWCNT-EDA/EP/PC nanocomposite and at $T_{onset} = 447$°C and $T_d = 507$°C for the 2 wt % MWCNT-EDA/EP/PC nanocomposite. In the 2 wt % EP-coated MWCNT, the T_{onset} for the samples containing MWCNT-EDA increased by only 3°C whereas T_d has increased by as much as

Table I. Characteristic Temperatures of Thermal Degradation of PC Nanocomposites

Samples	T_{onset} (°C)	$T_{degradation}$ (°C)
Pristine PC	430	456
2 wt % MWCNT/PC	443	464
2 wt % MWCNT-EP/PC	444	464
1.5 wt % MWCNT-EDA/EP/PC	445	502
2 wt % MWCNT-EDA/EP/PC	447	507
1.5 wt % Ag/MWCNT-EDA/EP/PC	473	516
2 wt % Ag/MWCNT-EDA/EP/PC	489	521

43°C with respect to samples containing MWCNT–COOH. This suggests a strong interaction between the three phases (MWCNT-EDA, EP, and PC), which was further supported by the Fourier transform infrared (FTIR) analysis described in our previous study.[9] The amine group of EDA formed an electrostatic ionic bond with the sulphonyl group of PEDOT : PSS. The electron-rich nitrogen of the amine group was converted into cationic radical NH_3^+ due to the extraction of hydrogen from the sulphonyl group of PEDOT : PSS, which further electrostatically bonded with SO_3^- of PEDOT : PSS.[18] Eventually, functionalization of diamine on MWCNT leads to the formation of strongly bonded MWCNT-EDA/EP/PC assembly, shifting the T_d of MWCNT-EDA/EP/PC to the higher temperature.

Finally, we explored the thermal degradation behavior of our final configuration that added Ag nanoparticles to the nanocomposite system. Figure 5(c) shows the thermal stability of PC nanocomposites with 1.5 and 2 wt % Ag/MWCNT-EDA/EP fillers. Again, we observed an initial decrease of 4 wt % in weight in the range of 200–400°C due to the decomposition of EDA. There was an increase in T_{onset} due to the polymer chain mobility reduction caused by the entanglement with MWCNTs. The degradation profile widened and there was an increase in T_d caused by the addition of EDA. In particular, the addition of Ag nanoparticles resulted in the T_{onset} and T_d to be increased by 42 and 14°C as compared to the 2 wt % MWCNT-EDA/EP/PC nanocomposite [Figure 5(b)]. In total, the combined effects of 2 wt % Ag/MWCNT-EDA/EP increased the T_{onset} and T_d of pristine PC by 59 and 65°C, respectively. One of the mechanisms in which Ag is able to increase the thermal stability of the nanocomposite is because of the additional number of hydrogen bonds between EP and PC as compared to the MWCNT-EP/PC and MWCNT-EDA/EP/PC samples. In our previous work,[9] we showed that Ag nanoparticles can segregate PEDOT : PSS linkages. Here, we present further evidence of this by studying the thermal degradation of Ag/EP compared to PEDOT : PSS as shown in Figure 5(d). The thermal degradation of PEDOT : PSS has a three-step degradation profile. The T_d peak observed at 65°C is attributed to the water release. The second T_d at 322°C indicates the loss of the sulphonyl group of the PSS chains. Finally, the rupture of the PEDOT : PSS backbone happens at around $T_d = 384$°C. However, the 17 wt % Ag/PEDOT : PSS sample has a very different degradation profile. First, the absence of the first peak, corresponding to the loss of water, is because the specimen was dried in a vacuum oven during preparation. Secondly, the T_d peaks associated with the loss of the sulphonyl group of the PSS chains and the rupture of the PEDOT : PSS backbone are lowered to 262°C and 350°C, respectively. This is an indication of how the Ag nanoparticles decrease the strength of the PEDOT : PSS bonds and segregate the PEDOT : PSS linkages. Thus, the Ag/MWCNT-EDA/EP filler, with numerous hydrogen bonds to PC, acts as a dense barrier layer that improves the overall thermal stability of the material. Charactetristic temperatures of the thermal degradation all formulations are listed in Table I.

DSC Analysis of PC Nanocomposites

Figure 6(a) shows the DSC thermograms of PC and MWCNT-EDA/EP/PC nanocomposites with different concentrations of the two-phase filler. Clearly, there is decrease in the glass transition temperature (T_g) with respect to the filler content. T_g decreased from 150.5°C to 138.2°C with the maximum concentration of 2 wt % MWCNT-EDA/EP. Although it has been

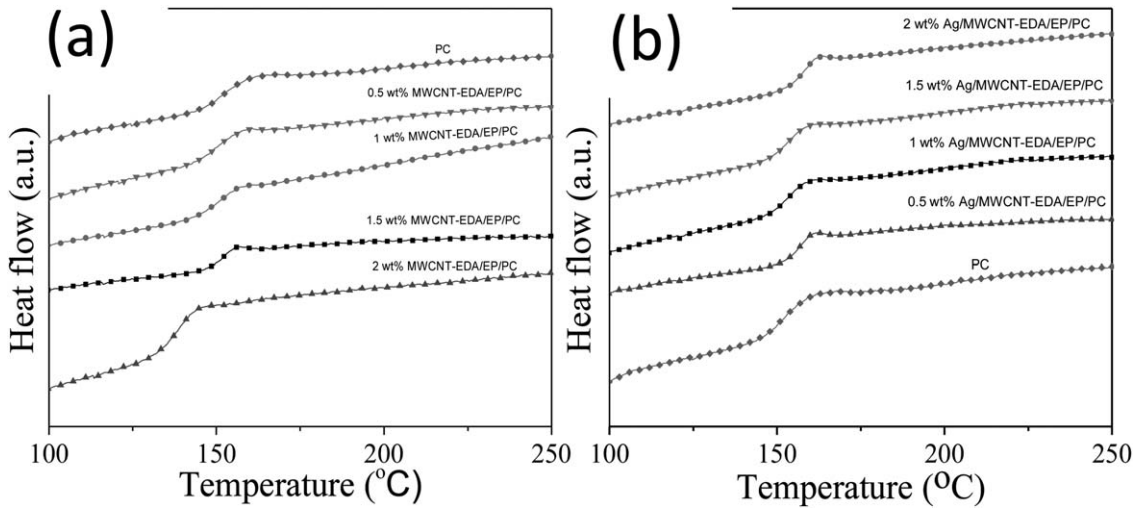

Figure 6. DSC thermograms of (a) MWCNT-EDA/EP/PC nanocomposites and (b) Ag/MWCNT-EDA/EP/PC nanocomposites. [Color figure can be viewed in the online issue, which is available at wileyonlinelibrary.com.]

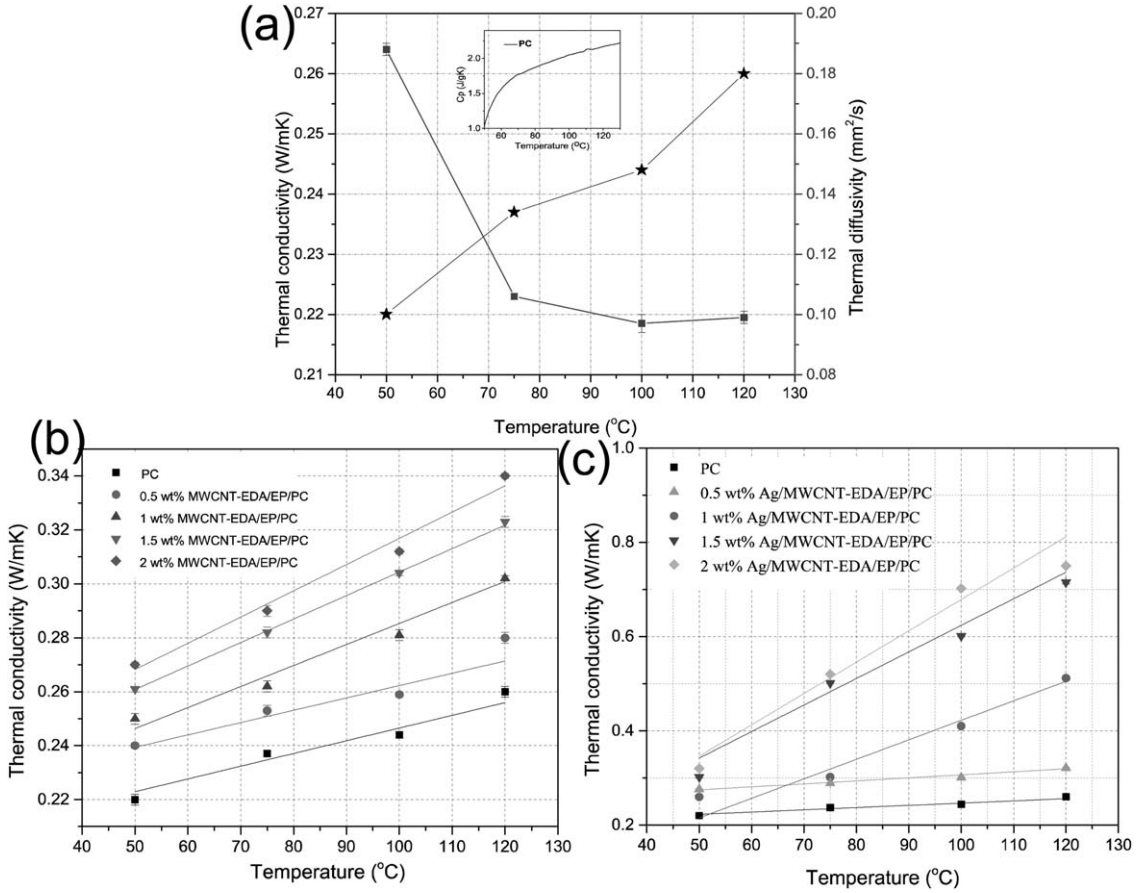

Figure 7. Thermal conductivity of PC and PC nanocomposites (a) the thermal conductivity and thermal diffusivity of pristine PC; (b) the thermal conductivity of MWCNT-EDA/EP/PC nanocomposites, and (c) thermal conductivity of Ag/MWCNT-EDA/EP/PC nanocomposites. [Color figure can be viewed in the online issue, which is available at wileyonlinelibrary.com.]

reported[19] that MWCNTs are able to restrict the slippage between molecular chains, in this case, the presence of the conductive polymer coating surrounding the nanofillers dominates the chain kinetics. This is consistent with our previous results[1] in which we identify that EP acts as an antiplasticizer into PC, reducing the glass transition temperature. Another possible mechanism for the decrese in T_g is the availability of bulky PEDOT : PSS groups in between the matrix polymer chains. EP consists of a long PSS chain and a bulky PEDOT oligomer, in which PEDOT is electrostatically attached to PSS.[20] The

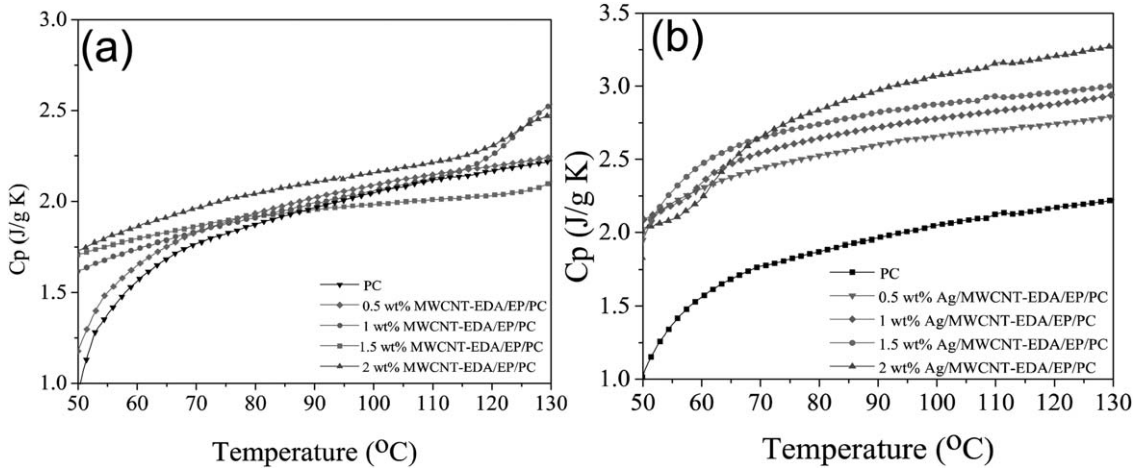

Figure 8. Specific heat of (a) MWCNT-EDA/EP/PC and (b) Ag/MWCNT-EDA/EP/PC nanocomposites. [Color figure can be viewed in the online issue, which is available at wileyonlinelibrary.com.]

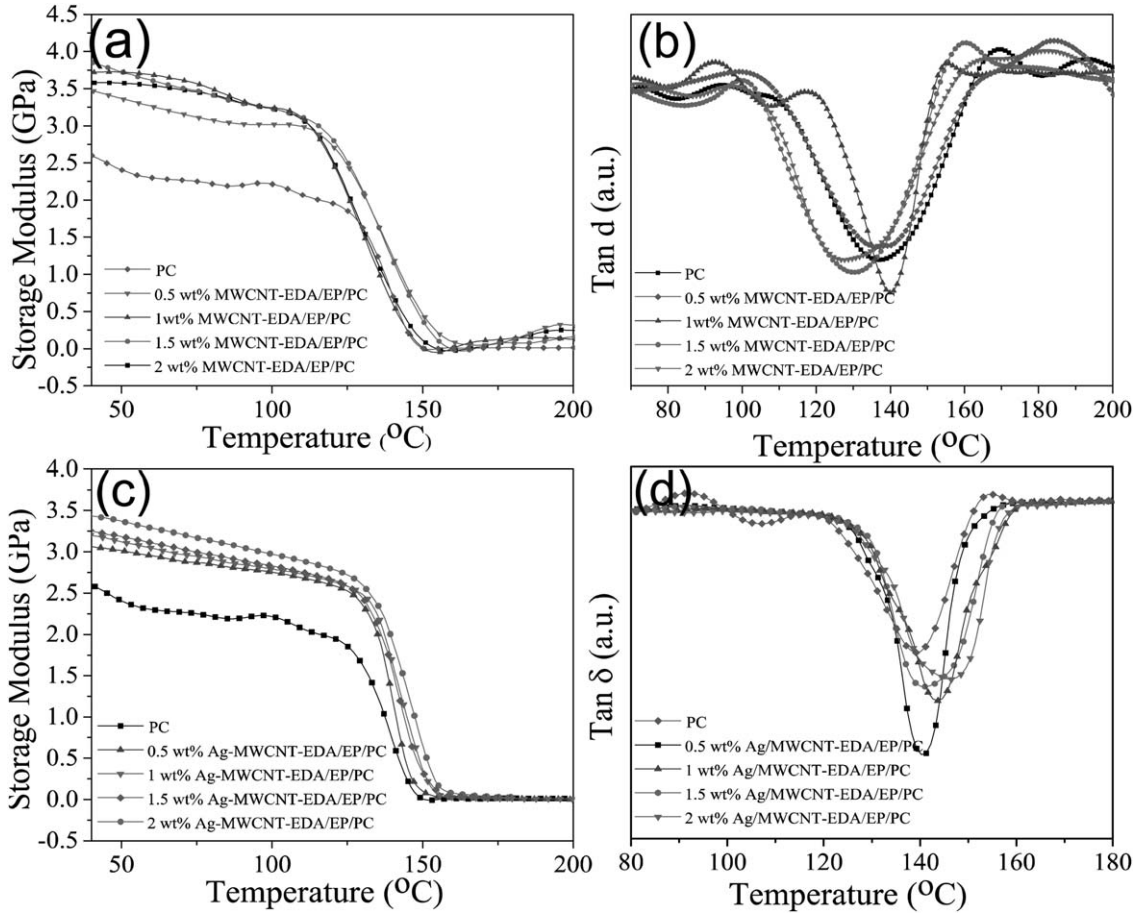

Figure 9. Dynamic mechanical properties of MWCNT-EDA/EP/PC and Ag/MWCNT-EDA/EP/PC nanocomposites: (a) and (c) storage modulus, (b) and (d) damping factor. [Color figure can be viewed in the online issue, which is available at wileyonlinelibrary.com.]

hydrogen bond between EP and PC was formed through $-SO_3H$ of PSS and –CO of PC.[1] This hydrogen bond makes the connection between EP and PC strong. But, the presence of bulky PEDOT in EP lowers the intermolecular forces of the PC chains in the matrix, resulting in the softening of the PC chains at a lower temperature.[20]

Figure 6(b) shows the thermograms for the three-phase filler nanocomposites with different concentrations of Ag/MWCNT-EDA/EP. Contrary to the previous case, the T_g of these nanocomposites increases as the amount of filler increases. For example, the T_g of 2 wt % Ag/MWCNT-EDA/EP/PC increased to 157°C from the original 150.55°C of pure PC. This change suggests a strong interfacial compatibility of the fillers with the matrix. Two mechanisms were proposed for such a change: Firstly, as mentioned before, Ag nanoparticles can segregate the PEDOT : PSS linkage. The smaller molecular groups attached to the PC therefore reduce the distances between PC chains as compared with bulky PEDOT : PSS. Secondly, the larger amount of interactions between EP and PC become hurdles to segmental mobility of PC chains.

Thermal Conductivity

We used eq. (1) to measure the thermal conductivity of PC and PC nanocomposites. The *Cp*, α, and ρ of PC, and PC nanocomposites are required to determine the thermal conductivity (K) using eq. (1). We select the temperature range of 50–120°C for the measurement of α, which is below the T_g of PC, because thermal conductivity and Cp for polymers behave anomalously above the T_g.[14] Figure 7(a) shows Cp, α, and K with temperature for PC, indicating that α decreased with temperature, whereas the thermal conductivity and Cp increased with temperature. Figure 7(b) shows the thermal conductivity of MWCNT-EDA/EP/PC with respect to temperature with the different concentrations of MWCNT-EDA/EP (graphs for Cp with respect to temperature are provided in Figure 8(a)). The thermal conductivity for the nanocomposites increases with the MWCNT-EDA/EP content and temperature. At 50°C, the thermal conductivities of 0.5 wt % MWCNT-EDA/EP/PC and 2 wt % MWCNT-EDA/EP/PC are 0.24 and 0.28 W/mK, respectively, which increased up to 0.27 and 0.34 W/mK, respectively, at 120°C.

On the other hand, Figure 7(c) shows the thermal conductivity of Ag/MWCNT-EDA/EP/PC nanocomposites as a function of temperature with different concentrations of Ag/MWCNT-EDA/EP (the Cp graph as a function of temperature is provided in Figure 8(b)).

As before, the thermal conductivity for the nanocomposites increases as the Ag/MWCNT-EDA/EP content and temperature

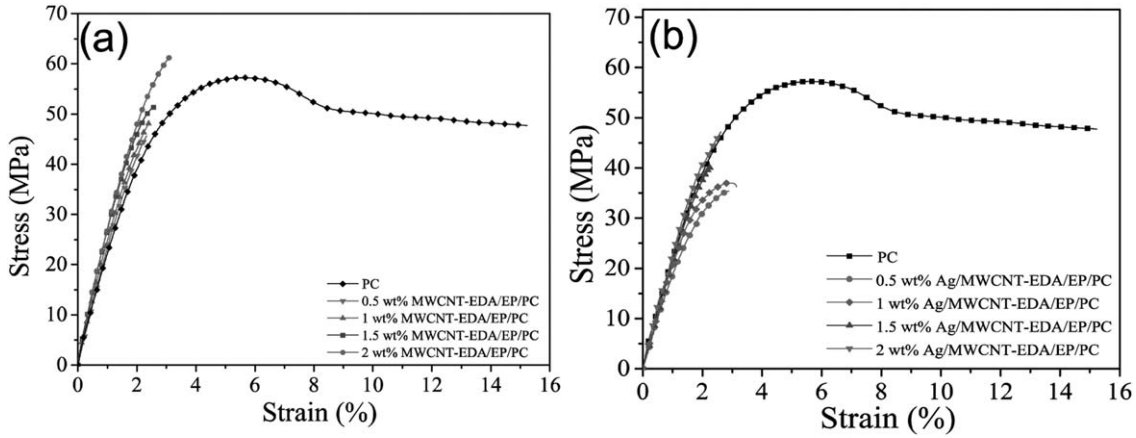

Figure 10. Stress–strain curves of (a) MWCNT-EDA/EP/PC nanocomposites and (b) Ag/MWCNT-EDA/EP/PC nanocomposites. [Color figure can be viewed in the online issue, which is available at wileyonlinelibrary.com.]

increase. Moreover, as the concentration of Ag/MWCNT-EDA/EP increases, the dependence on temperature grows stronger. For example, at 50°C, the thermal conductivity is around 0.3±0.03 W/mK for all Ag/MWCNT-EDA/EP/PC configurations. At 120°C, the thermal conductivity of the 2 wt % Ag/MWCNT-EDA/EP/PC sample is 0.75 W/mK, which is an increase of 120% compared with the initial value. In comparison, K of 0.5 wt % Ag/MWCNT-EDA/EP/PC at 120°C is only 0.32 W/mK. A comparison of this set of samples to those in Figure 7(b) reveals that the strong temperature dependence effect is clearly related to the presence of Ag nanoparticles. As explained previoulsy,[1] the relatively low improvement in thermal conductivity of EP-coated-MWCNT/PC nanocomposites with respect to MWCNT content is due to the low thermal conductivity of PEDOT/PSS, which acts as a buffer zone for the phonon scatter in the network of highly conductive MWCNTs. In Ag/MWCNT-EDA/EP/PC samples, the presence of Ag introduces electrons as a new type of thermal transport carrier in the nanocomposites. Since the thermal conductivity of Ag is nearly constant in the range of temperature studied, we posit that, as the temperature rises, the scattering between phonons and electrons diminishes, allowing the electrons to play a more significant role in the overall thermal conductivity of the nanocomposite.[21] Overall, EP, Ag nanoparticles, and MWCNT-EDA used together offer the possibility of thermally conducting PC nanocomposites compared with MWCNT/EP/PC nanocomposites.[1]

Dynamic Mechanical Properties

Figure 9 shows the change in the storage modulus and related tan δ of PC nanocomposites as a function of temperature with different concentrations of MWCNT-EDA/EP and Ag/MWCNT-EDA/EP fillers. As expected form a thermoplastic material, the storage modulus of all samples decreases as the temperature increases. The glass transition temperature, Tg, is observed as a peak in the tan δ curve, which corresponds to a sharp decrease in the storage modulus. Figure 9(a,b) show the MWCNT-EDA/EP/PC samples. Generally, MWCNT-EDA/EP/PC nanocomposites have improved storage moduli both in the glassy region and in the rubbery region compared with pristine PC and their glass transition temperature decreases with respect to the MWCNT concentration. The storage modulus for MWCNT-EDA/EP/PC samples at room temperature has a maximum value of 3.85 GPa at 1.5 wt % filler loading. With higher filler concentration, the storage modulus slightly decreases. This trend was also observed when measuring the Young's modulus at room temperature from simple mechanical loading [Figure 10(a,b)]. These results indicate that the state of dispersion is

Table II. Mechanical Properties of PC Nanocomposites

Sample	Tg (by DSC)	Tg (by DMA)	Storage modulus		Youngs modulus (Gpa)	Tensile strength (Mpa)
			E′max (Gpa)	E'_{Tg} (Gpa)		
Pristine PC	150.55	139.2	2.60±0.08	0.76±0.06	2.0±0.06	57.47
0.5 wt % MWCNT-EDA/EP/PC	147	137.0	3.46±0.07	1.41±0.09	2.5±0.07	45.65
1 wt % MWCNT-EDA/EP/PC	146	134.12	3.85±0.05	1.60±0.09	2.7±0.05	48.36
1.5 wt % MWCNT-EDA/EP/PC	146.25	129	3.72±0.10	2.12±0.07	2.9±0.04	51.58
2 wt % MWCNT-EDA/EP/PC	138.23	126.1	3.58±0.08	2.39±0.10	2.0±0.08	61.47
0.5 wt % Ag/MWCNT-EDA/EP/PC	151.17	138.62	3.06±0.09	1.40±0.09	2.1±0.08	35.49
1 wt % Ag/MWCNT-EDA/EP/PC	152	140.4	3.19±0.05	1.51±0.10	2.2±0.07	36.61
1.5 wt % Ag/MWCNT-EDA/EP/PC	153	142.0	3.25±0.04	1.46±0.09	2.3±0.04	39.98
2 wt % Ag/MWCNT-EDA/EP/PC	157	145.0	3.44±0.07	1.22±0.08	2.5±0.05	47.25

optimum at around 1 wt %. The relevant measurements from the DMA and the simple tensile testing are given in Table II. The increase in the storage modulus and the decrease in the glass transition temperature is in agreement with our previous characterization[1] in which EP coated –COOH functionalized MWCNTs were used instead. This is ascribed to the antiplasticization effect of PEDOT : PSS in PC.

Figure 9(c,d) show the DMA results for Ag/MWCNT-EDA/EP/PC nanocomposites. In comparison, the addition of Ag introduces two main differences with respect to the previous configuration: (1) The results show a clear trend of decreasing storage modulus at room temperature. The same trend is also observed from the Young's modulus measurements from simple tensile testing shown in Figure 10. (2) The glass transition temperature shifted to a higher temperature as was previously observed during the DSC analysis and explained in terms of the increased number of electrostatic interactions between the segregated PEDOT : PSS molecules and the PC chains.

CONCLUSIONS

In this article, we explored if a hybrid three-phase filler could improve the thermal properties of PC nanocomposites. PEDOT : PSS, Ag nanoparticles and MWCNT-EDA were used to form PEDOT : PSS coated Ag nanoparticles on MWCNTs. It was then loaded into PC nanocomposites.

Our results confirm that the PEDOT : PSS-coated Ag nanoparticles on MWCNTs segregates bulky PEDOT from PEDOT : PSS. This process allows a strong interaction of the three-phase filler with the PC matrix, resulting in improved thermo mechanical performance and higher thermal stability. In particular, it is interesting to note that the samples containing Ag/MWCNT-EDA/EP were able to reverse the glass transition temperature trend that was found in samples containing only MWCNT-EDA/EP. We also observed that the thermal conductivity of PC composites increased with the addition of three-phase fillers and that the prescence of Ag nanoparticles produced a stronger temperature dependence.

This three-phase conductive filler can be used as a potential material to tailor a variety of thermally stabilized engineering materials for different applications.

ACKNOWLEDGMENTS

Funding for this work was provided from King Abdullah University of Science and Technology (KAUST) baseline fund. The authors are grateful to KAUST for its financial support.

REFERENCES

1. Zhou, J.; Ventura, I. A.; Lubineau, G. *Ind. Eng. Chem. Res.* **2014**, *53*, 3539.
2. Zhou, J.; Lubineau, G. *ACS Appl. Mater. Interface.* **2013**, *5*, 6189.
3. Chen, J.; Lu, H.; Yang, J.; Wang, Y.; Zheng, X.; Zhang, C.; Yuan, G. *Compos. Sci. Technol.* **2014**, *94*, 30.
4. Dai, Z. H.; Gao, Y.; Liu, L.; Poetschke, P.; Yang, J.; Zhang, Z. *Polymer* **2013**, *54*, 3723.
5. Hasell, T.; Lagonigro, L.; Peacock, A. C.; Yoda, S.; Brown, P. D.; Sazio, P. J. A.; Howdle, S. M. *Adv. Funct. Mater.* **2008**, *18*, 1265.
6. Wold, C.; Grampel, R. *Polym. Test.* **2009**, *28*, 495.
7. Choi, W. S.; Ryu, S. H. *Colloids Surf. A* **2011**, *375*, 55.
8. Panayiotis, B.; Dimitrios, K.; Apostolos, A.; Georgios, S. *RSC Adv.* **2014**, *4*, 2911.
9. Patole, A.; Lubineau, G. *Carbon* **2015**, *81*, 710.
10. Raza, R.; Saqib, A.; Fiaz, A.; Shafiq, U.; John, T. G. *Polym. Compos.* **2014**, *35*, 1807.
11. Grinou, A.; Bak, H.; Young, S.; Jin, H. J. *J. Dispersion Sci. Technol.* **2011**, *33*, 750.
12. Zhong, J. S.; Hu, J.; Cai, W.; Yang, F.; Liu, L.; Liu, H.; Yang, X.; Liang, X.; Xiang, W. *J. Alloys Compd.* **2010**, *501*, L15.
13. Neelgund, G. M.; Oki, A. *J. Nanosci. Nanotechnol.* **2011**, *11*, 3621.
14. Parker, W. J.; Jenkins, R. J.; Butler, C. P.; Abbot, J. L. *J. Appl. Phys.* **1961**, *32*, 1679.
15. Oneill, M. J. *Anal. Chem.* **1966**, *38*, 1331.
16. Tang, H.; Chen, J. H.; Huang, Z. P.; Wang, D. Z.; Ren, Z. F.; Nie, L. H.; Kuang, Y. F.; Yao, S. Z. *Carbon* **2004**, *42*, 191.
17. Wang, S. F.; Hu, Y.; Wang, Z.; Yong, T.; Chen, Z.; Fan, W. *Polym. Degrad. Stab.* **2003**, *80*, 157.
18. Sakaguchi, R. L.; Shah, N. C.; Lim, B. S.; Ferracane, J. L.; Borgersen, S. E. *Dent. Mater.* **2002**, *18*, 197.
19. Andrews, R.; Weisenberger, M. C. *Curr. Opin. Solid State Mater. Sci.* **2004**, *8*, 31.
20. Jackson, W. J.; Caldwell, J. R. *J. Appl. Polym. Sci.* **1967**, *11*, 211.
21. Touloukian, Y. S.; Powell, R. W.; Ho, C. Y.; Klemens, P. G. In Thermophysical Properties of Matter – The TPRC Data Series; Thermal Conductivity – Metallic Elements and Alloys, IFI/Plenum: New York, Vol. 1; **1970**.